SHARMA, G. L. (1980). PhD thesis, IIT Delhi, India.
SINGH, K. & TRIGUNAYAT, G. C. (1989*a*). *Phase Transit.* **16/17**, 529–535.
SINGH, K. & TRIGUNAYAT, G. C. (1989*b*). *J. Cryst. Growth*, **97**, 863–865.
SOUDMAND, M. & TRIGUNAYAT, G. C. (1989). *Phase Transit.* **16/17**, 417–424.
TAIROV, Y. M. & TSVETKOV, V. F. (1983). *Crystal Growth and Characterization of Polytype Structures*, edited by P. KRISHNA, pp. 111–161. Oxford: Pergamon Press.
TRIGUNAYAT, G. C. (1971). *Phys. Status Solidi A*, **4**, 281–303.
TRIGUNAYAT, G. C. & VERMA, A. R. (1976). In *Physics and Chemistry of Materials with Layered Structures*, Vol. 2, edited by F. LEVY. Dordrecht: Reidel.
TYAGI, U. P. & TRIGUNAYAT, G. C. (1986). *Cryst. Res. Tech.* **21**, 891–895.
TYAGI, U. P. & TRIGUNAYAT, G. C. (1987). *Acta Cryst.* A**43**, C-309.
TYAGI, U. P. & TRIGUNAYAT, G. C. (1988). *Acta Cryst.* C**44**, 1157–1162.

Acta Cryst. (1993). B**49**, 458–463

Small-Angle X-ray Scattering Study of Precipitation in a Cu–2 at.% Co Alloy

BY P. ANCRENAZ

Centre de Recherches et Etudes d'Arcueil, 16 *bis Avenue Prieur de la Côte d'Or*, 94114 *Arcueil CEDEX*, *France*

C. SERVANT

Laboratoire de Métallurgie Structurale, *UA CNRS* 1107, *Université de Paris-Sud*, *Bâtiment* 413, 91405 *Orsay CEDEX*, *France*

AND O. LYON

Laboratoire pour l'Utilisation du Rayonnement Electromagnétique, *Université de Paris-Sud*, *Bâtiment* 209, 91405 *Orsay CEDEX*, *France*

(*Received* 30 *December* 1991; *accepted* 29 *October* 1992)

Abstract

The unmixing at 923 K of a binary alloy Cu–2 at.% Co was studied by anomalous small-angle X-ray scattering performed at the Co *K*-absorption edge and transmission electron microscopy. For ageings of 3 and 120 h a marked anomalous effect was observed. Experimental curves were fitted with the help of a model that took into account the radius of precipitates, their volume fraction and the radius of excluded spheres. X-ray absolute scattered-intensity measurements allowed us to determine the cobalt concentration in precipitates.

1. Introduction

The Cu–Co binary system is difficult to investigate by the classical small-angle X-ray scattering technique due to the very small difference in atomic number between Cu and Co. To increase the contrast, use can be made of the anomalous effect.

The present study aims at determining the different stages of the unmixing of a Cu–2 at.% Co alloy aged at 923 K for different ageing times by the anomalous small-angle X-ray scattering technique (ASAXS) performed at the Co *K* edge and transmission electron microscopy (TEM).

2. Experimental procedure

2.1. *Sample preparation and heat treatment*

The Cu–2 at.% Co alloy becomes single phased by homogenization treatment at 1238 K for 2 h under an argon atmosphere, followed by water quenching. Precipitation was performed at 923 K, under an argon atmosphere, for an ageing time varying between $\frac{1}{2}$ and 120 h.

The thin foils used both for ASAXS experiments and for TEM observations were obtained from samples by electrothinning. Final thickness was about 15 to 25 μm. Polishing was carried out at 293 K in a solution containing 30 cm^3 pure water and 70 cm^3 orthophosphoric acid, with a potential difference of 1 V.

2.2. *TEM*

The TEM and microdiffraction experiments were carried out with a JEOL 120C microscope operating at 120 kV.

0108-7681/93/030458-06$06.00

2.3. *ASAXS apparatus*

The ASAXS experiments were carried out at LURE (Laboratoire pour l'Utilisation du Rayonnement Electromagnétique, Orsay, France) on the D22 beam line, below the Co K-absorption edge ($\lambda_K = 0.1608$ nm, $E = 7708$ eV) to reduce the Co atomic scattering factor due to the 'anomalous effect'. On the D22 beam line, the whole X-ray beam path is in a vacuum to minimize the parasitic scattering by air. The primary-beam intensity I_0 was monitored by an upstream scintillator. The scattered-beam intensity was recorded by a position-sensitive detector.

2.4. *Treatment of data*

The data were corrected only for background and absorption. We used the classical correction formula (Bouzid, Servant & Lyon, 1988),

$$I(q,E) = \varepsilon_d(q)\varepsilon_d(E)t^{-1}\{[I_{\text{sample}}/I_0T(E)] - [I_{\text{parasitic}}/I_0'T'(E)]\}. \quad (1)$$

The sample thickness t was determined from transmission measurements $T(E)$ at different energies E by use of corresponding data for the absorption coefficients. The precision for the thickness t was about 3%. The detector efficiencies $\varepsilon(q)$ and $\varepsilon(E)$ as a function of position and energy were determined previously.

3. Anomalous small-angle X-ray study

3.1. *Theory*

The aged binary Cu–2 at.% Co alloy comprises cobalt-rich precipitates in a copper matrix. The study of the cobalt precipitation is difficult because the difference between the atomic numbers of cobalt and copper is low ($Z_{Co} = 27$, $Z_{Cu} = 29$). The anomalous effect is useful in this case because the variation of X-ray beam energy can lead to an increase of the scattered intensity (Lyon, Hoyt, Pro, Davis, Clark, de Fontaine & Simon, 1985). The scattered intensity is a linear combination of partial structure functions (de Fontaine, 1979),

$$I(q,E) = \sum_{i,j=1}^{n} (f_i - f_0)_{(E)}(f_j - f_0)^*_{(E)}S_{ij}(q), \quad (2)$$

where $q = (4\pi\sin\theta)/\lambda$ is the magnitude of the reciprocal-space scattering vector and $S_{ij}(q)$ is the Fourier transform of the corresponding pair-correlation function. In general, f_i and f_j are the atomic scattering factors of the minor elements and f_0 is that of the major element. In the case of the Cu–2 at.% Co alloy, (2) becomes

$$I(q,E) = (f_{Co} - f_{Cu})_{(E)}(f_{Co} - f_{Cu})^*_{(E)}S_{CoCo}(q). \quad (3)$$

Table 1. *Anomalous correction for the atomic scattering factor of cobalt as a function of X-ray beam energy* (*Sasaki*, 1984)

	E (eV)	λ (nm)	f'	f''
Copper	7500	0.16529	−1.625	0.668
	7650	0.16205	−1.717	0.645
	7680	0.16142	−1.738	0.640
	7700	0.16100	−1.751	0.637
Cobalt	7500	0.16529	−3.367	0.496
	7650	0.16205	−4.599	0.480
	7680	0.16142	−5.359	0.476
	7700	0.16100	−6.670	0.474

In the immediate neighbourhood of an absorption edge, the atomic scattering factor changes and is written as

$$f(q,E) = Z^0(q) + f'(q,E) + if''(q,E). \quad (4)$$

The dependence on q of the X-ray atomic scattering factor is negligible at small angles and has been neglected. $Z^0(q)$ is the energy-independent part of this factor, $f'(q,E)$ is the real part of the anomalous correction, which is strongly dependent on the energy, and $f''(q,E)$ is the imaginary part.

Experiments have been performed with four different X-ray beam energies (7700, 7680, 7650 and 7500 eV), which lead to a significant variation of the scattering factor (Table 1).

3.2. *ASAXS results*

Two states of the Cu–2 at.% Co alloy aged at 3 and 120 h were studied.

3.2.1. *Alloy aged for* 3 h. The scattering curves are reported in Fig. 1. We observed a marked anomalous effect. The scattered intensity increases with the increasing energy of the X-ray beam. These curves have a maximum of strong intensity. The position of this maximum ($q = 0.12$ nm^{-1}) does not change with the value of the beam energy. Also, these curves have a second maximum for $q = 0.50$ nm^{-1} (Fig. 1). There are two possible explanations for this second maximum: either a second type of precipitates exist or the scattering function of spherical precipitates leads to the observation of several maxima because their size distribution is very small.

In this application, the curves were calculated with the help of a model that simulates the monodispersion of spherical precipitates in the case of a binary alloy (Hennion, Ronzaud & Guyot, 1982).

The expression for the scattered intensity $I(q,E)$ is

$$I(q,E) = AN_vV_p^2[\langle F_p(q)^2\rangle - \langle F_p(q)\rangle^2|1 - I'(q,N_v,D)|], \quad (5)$$

where N_v is the number of scattering precipitates per unit volume, V_p is the precipitate volume, $I'(q,N_v,D)$ is the interference function of scattered waves by the precipitates defined by Ashcroft & Lekner (1966) and D is the diameter of the excluded spheres. $\langle F_p(q)\rangle$ is

the scattering function of a spherical precipitate with radius R,

$$\langle F_p(q)\rangle^2 = \langle F_p(q)^2\rangle = F_p(q)^2 = 9(\sin qR - qR\cos qR)^2/(qr)^6. \quad (6)$$

The agreement between the experimental and the fitted curves is good (Fig. 2). The second maximum observed experimentally is indeed calculated by this model. The second maximum is typical of a condensed system containing precipitates whose size dispersion is very small and there is therefore only one type of precipitate. The calculated values of R, D and N_v are reported in Table 2.

The calculated value of the scattered intensity is equal to zero just before the second maximum, which occurs at $q = 0.50\ \text{nm}^{-1}$, but the experimental data do not have this minimum because the size dispersion of the precipitates is not small enough and experimental collimation of the X-ray beam is not strictly a pinhole.

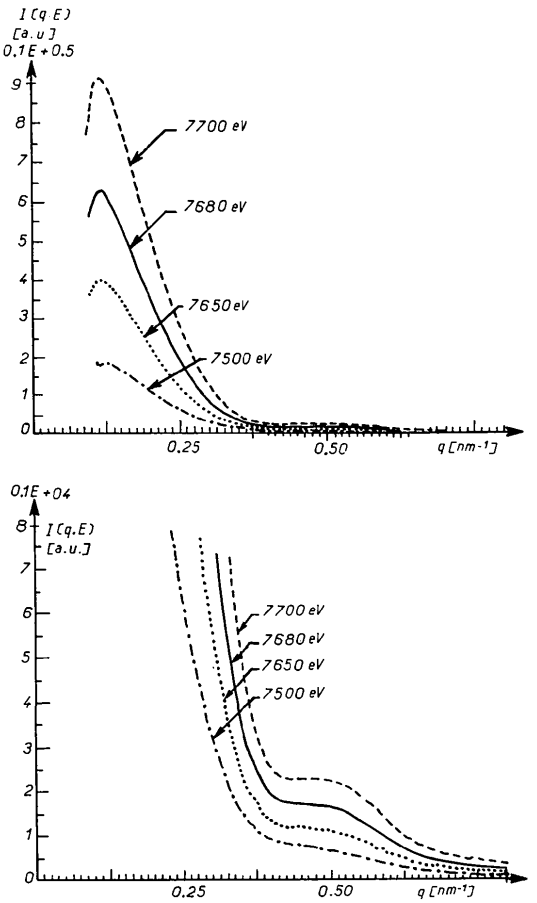

Fig. 1. ASAXS curves of the Cu–2 at.% Co alloy aged at 923 K for 3 h, recorded at X-ray energies increasing from 7500 to 7700 eV.

Table 2. *Fitted parameters for samples aged at* 923 K *for* 3 *and* 120 h

Ageing time (h)	3	120
R (nm)	10.7	25.0
N_v (cm^{-3})	3.83×10^{15}	4.1×10^{14}
D (nm)	34.8	50.2
Volume fraction	0.020	0.027

3.2.2. *Alloy aged for* 120 h. For this time, a very marked anomalous effect was observed (Fig. 3). No maximum is noted on the scattering curves because of the experimental conditions used; in fact, it is not possible to measure the scattered intensity for q values lower than $0.075\ \text{nm}^{-1}$. However, previous small-angle neutron scattering experiments have shown this maximum for $q = 0.04\ \text{nm}^{-1}$ (Ancrenaz & Servant, 1992). The second maximum observed in the case of the 3 h ageing is not observed for the 120 h ageing. Use of the model leads to reasonable agreement with the experimental data (Fig. 4). The more significant dispersion in the precipitate size than in the alloy aged for 3 h leads to the loss of the second maximum. Furthermore, the agreement between the calculated curve and the experimental data is less satisfactory than for the alloy aged for 3 h.

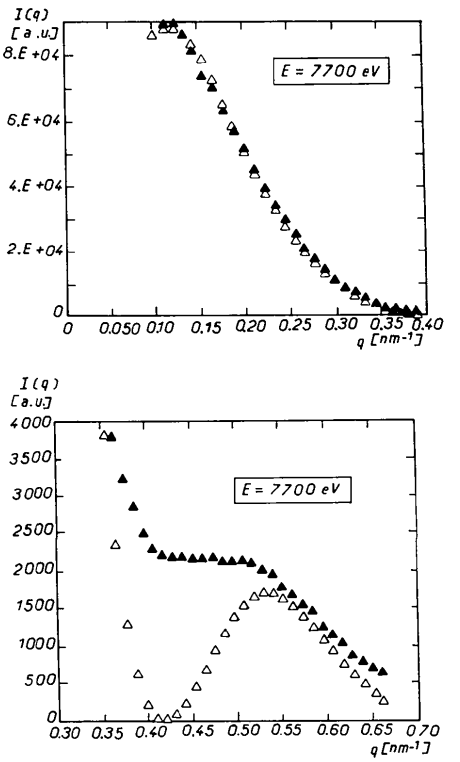

Fig. 2. Experimental and fitted curves of the alloy aged at 923 K for 3 h; ASAXS curves recorded at 7700 eV.

4. Kinetics of precipitate coarsening

4.1. *Two-phase model*

The application of the law of Guinier & Fournet (1955) to that part of the scattering curve after the first maximum allows the estimation of the precipitate size. The shape of the scattering curve is related to the radius of gyration of the precipitate (R_g) having a volume V_p and is approximated by an exponential expression according to

$$I(q) \propto (\rho - \rho_0)^2 V_p^2 \exp(-q^2 R_g^2/3). \quad (7)$$

This approximation is valid if the scattering precipitates are widely separated and identical and if $qR_g < 1$. In the case of spherical precipitates, the relation between the precipitate radius (the Guinier radius, R_G) and the radius of gyration is simple,

$$R_G = (5/3)^{1/2} R_g. \quad (8)$$

The Guinier radius was calculated for different ageing times (Fig. 5). There is a change of slope for an ageing time of about 3 h, which indicates that there are two different stages of coarsening kinetics. The evolution of the precipitate radius with ageing time can be described by the relation $R_g \propto t^n$, where t is the ageing time. For an ageing time of 3 h, the steady state is reached, as assumed in the LSW theory (Lifshiftz & Slyozov, 1961) and n is equal to $0.28 \simeq \frac{1}{3}$. The same results were obtained from small-angle neutron scattering experiments and discussed as a function of data of different authors (Ancrenaz & Servant, 1992). Hence, the coarsening kinetics of cobalt precipitates seems to be controlled by cobalt diffusion in the copper matrix.

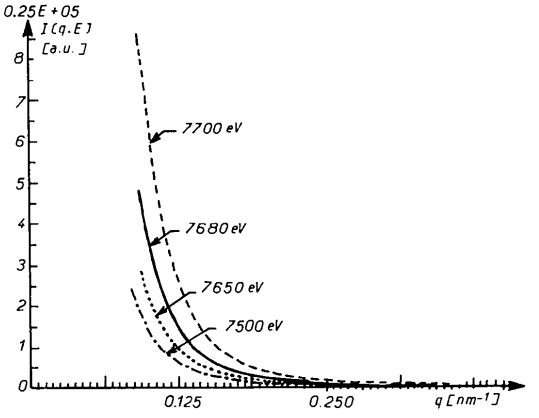

Fig. 3. ASAXS curves of the Cu–2 at.% Co alloy aged at 923 K for 120 h, recorded at X-ray energies increasing from 7500 to 7700 eV.

4.2. *Scaling analysis*

The unmixing of the Cu–2 at.% Co alloy was followed by the calculation of the two first moments $\tilde{q}_1$ and $\tilde{q}_2$, according to

$$\tilde{q}_n = \sum_{q_1}^{q_2} q^n S(q,t) / \sum_{q_1}^{q_2} S(q,t). \quad (9)$$

To represent $S(q,t)$, the Fourier transform of the pair-correlation function, we chose $I(q,t)$, which is directly proportional to $S(q,t)$. It is then easy to calculate the ratio

$$r = \tilde{q}_2/(\tilde{q}_1)^2. \quad (10)$$

This ratio is approximately constant for ageing times greater than 2 h (Fig. 6). This means that the unmixing of the alloy has reached a steady state and the volume fraction of precipitates is practically constant as a function of increasing ageing time (Ancrenaz & Servant, 1992).

5. TEM results

The alloy aged for 3 h contains coherent precipitates of cobalt: in fact the precipitates present a diffraction contrast associated with the elastic strain field

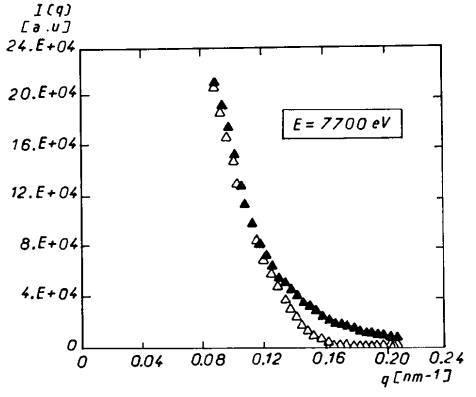

Fig. 4. Experimental and fitted curves of the Cu–2 at.% Co alloy aged at 923 K for 120 h; ASAXS curves recorded at 7700 eV.

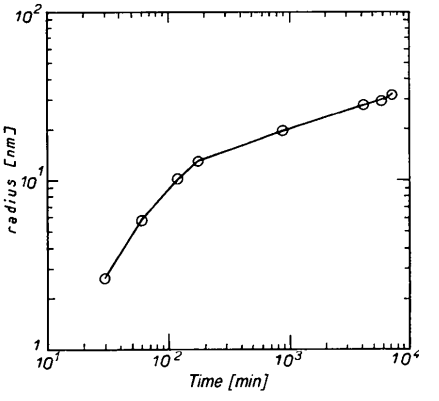

Fig. 5. Growth kinetics of precipitates in the Cu–2 at.% Co alloy aged at 923 K.

around them. This contrast presents a no-contrast line that is perpendicular to the operating reflection vector (Fig. 7).

After 120 h ageing time, the precipitates are semi-coherent and their shape is polyhedral (Fig. 8). During the ageing treatment, the precipitates become partially coherent because of coarsening. These precipitates present Moiré fringes and the lattice mismatch can be approximated with Moiré spacing measurement. Many interfacial dislocations are visible around the precipitates. These dislocations appear for the accommodation of the crystalline lattice between the precipitates and matrix.

It is impossible to distinguish the diffraction pattern of cobalt precipitates from that of the matrix because the crystallographic orientation and the structure of the precipitates are the same as those of the matrix and the cobalt atomic radius is close to that of copper ($r_{Co} = 0.126$, $r_{Cu} = 0.127$ nm).

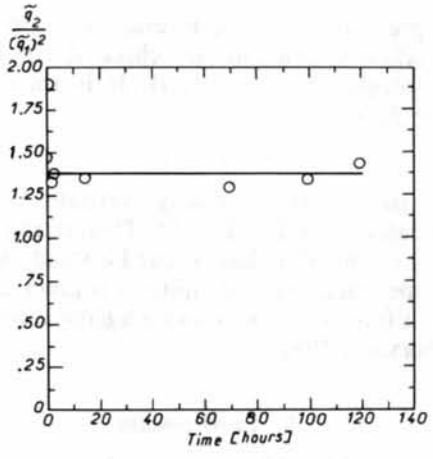

Fig. 6. Evolution of the ratio $r = \tilde{q}_2/(\tilde{q}_1)^2$ as a function of ageing time.

6. Composition of precipitates

The scattered intensity is directly proportional to the electron density difference between precipitates and matrix. It is thus possible to calculate the cobalt concentration of the precipitates if the absolute scattered intensity is measured with the help of a reference, Ni in this case. The expression of the absolute scattered intensity is

$$I_s = (f_{Co} - f_{Cu})^2 N_v (V_p)^2 (v_a)^{-1} (c_p - c_m)^2 \Sigma(q), \quad (11)$$

where N_v is the number of precipitates per unit volume, V_p the volume of precipitate, v_a the atomic volume, c_p the atomic cobalt concentration of the precipitate, c_m the atomic cobalt concentration of the matrix and $\Sigma(q)$ the scattering function of sphereical precipitates if the interference function is included.

The model described in § 3.2 is built according to the relation

$$I_s = A\Sigma(q). \quad (12)$$

The value of A is then easily determined since I_s is measured and $\Sigma(q)$ is fitted. With (11) and (12), we obtain

$c_p - c_m = 0.559$ for the 3 h ageing and
$c_p - c_m = 0.295$ for the 120 h ageing.

The equation for solute conservation is written as

$$f_v(c_p) + (1 - f_v)c_m = c_{Co} = 0.02, \quad (13)$$

where f_v is the volume fraction of the precipitates. The calculated atomic cobalt concentrations are

3 h ageing time: $c_p = 0.568$, $c_m = 0.009$;

120 h ageing time: $c_p = 0.313$, $c_m = 0.018$.

The cobalt concentration of precipitates exhibits a significant variation with the ageing time; in fact, the cobalt concentration for the 3 h ageing is twice that of the 120 h ageing. As we have seen in § 4.2, the

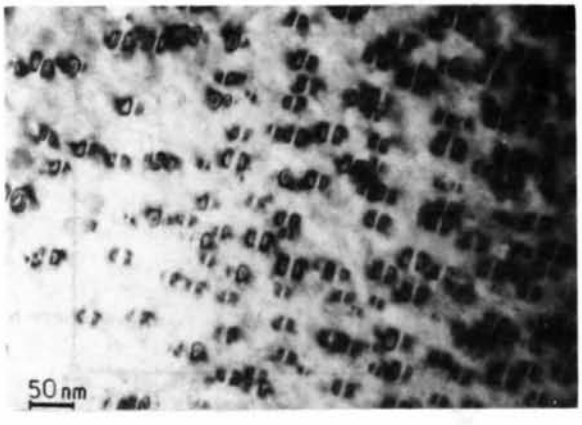

Fig. 7. Microstructure of the Cu–2 at.% Co alloy aged at 923 K for 3 h.

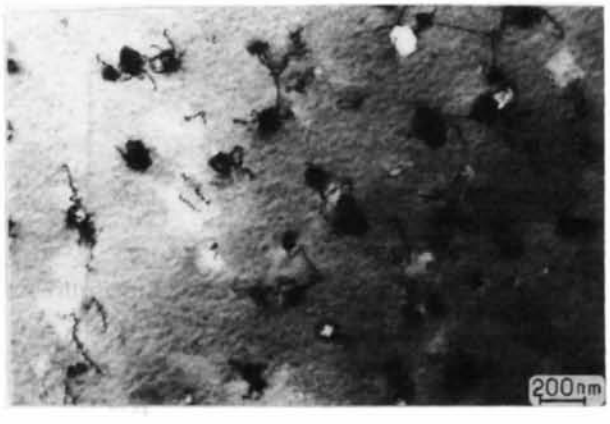

Fig. 8. Microstructure of the Cu–2 at.% Co alloy aged at 923 K for 120 h.

unmixing of the alloy reaches a steady state from about 3 h ageing time and the volume fraction of precipitates is practically constant with ageing time. However, the increase of ageing time leads to an important decrease in the cobalt concentration of precipitates.

7. Concluding remarks

ASAXS experiments have allowed the kinetic study of coarsening of the binary Cu–2 at.% Co alloy for ageing at 923 K. The cobalt precipitation is controlled by the cobalt diffusion in a copper matrix and a steady state is reached from about 3 h ageing time.

Spherical-precipitate simulation of almost size monodispersion is in good agreement with the experimental data for 3 h ageing time. After 120 h ageing, the size dispersion is more important and comparison between experimental and fitted data is not so good.

Determination of the cobalt concentration of precipitates was carried out with measurements of absolute scattered intensity. This concentration decreases when ageing time increases.

References

ANCRENAZ, P. & SERVANT, C. (1992). *J. Phys. (Paris) I*, **2**, 1113–1128.

ASHCROFT, N. M. & LEKNER, J. (1966). *Phys. Rev.* **145**, 83.

BOUZID, N., SERVANT, C. & LYON, O. (1988). *Philos Mag.* **57**, 343–359.

FONTAINE, D. DE (1979). *Solid State Physics*, Vol. 34, *Configurational Thermodynamics of Solid Solutions*, edited by E. SEITZ & D. H. TURNBULL, pp. 73–274. New York: Academic Press.

GUINIER, A. & FOURNET, G. (1955). *Small-Angle X-ray Scattering*. New York: John Wiley.

HENNION, M., RONZAUD, D. & GUYOT, P. (1982). *Acta Metall.* **30**, 599–610.

LIFSHIFTZ, I. M. & SLYOZOV, V. V. (1961). *J. Phys. Chem. Solids*, **19**, 35.

LYON, O., HOYT, J. J., PRO, D., DAVIS, B. E. C., CLARK, B., DE FONTAINE, D. & SIMON, J. P. (1985). *J. Appl. Cryst.* **18**, 480.

SASAKI, S. (1984). *Anomalous Scattering Factors for Synchrotron Radiation Users, Calculating using Cromer and Libermann Method*, pp. 22–83. National Laboratory for High Energy Physics, Ohomachi, Japan.

Acta Cryst. (1993). B**49**, 463–468

Thermal Effects in the Structure of Ammonium Perrhenate

BY BRIAN M. POWELL

AECL Research, Chalk River Laboratories, Chalk River, Ontario K0J 1J0, Canada

AND R. JULIAN C. BROWN, ANNE M. C. HARNDEN AND J. KIRK REID

Chemistry Department, Queen's University, Kingston, Ontario K7L 3N6, Canada

(*Received* 20 *July* 1992; *accepted* 1 *December* 1992)

Abstract

The structure of ND_4ReO_4 has been determined by neutron powder diffraction at 20 K intervals from 20 to 240 K and at 298 K. At 20 K the N—D bond distance is 1.025 (2) Å, the Re—O bond distance is 1.733 (2) Å and the D···O interionic distance is 1.878 (2) Å. The thermal expansion is normal at low temperatures, but becomes anomalous above about 90 K. The anion orientation changes by 3.2° over the whole temperature range while the cation orientation changes by 28°, and at the higher temperatures the deuterium thermal ellipsoid becomes highly elongated in the direction perpendicular to the N—D bond. This lends support to the pseudo-spin model for the anomalous behaviour of this salt, in which disorder between two non-equivalent orientations of the ammonium ion is assumed.

Introduction

Ammonium perrhenate crystallizes in the scheelite structure (tetragonal, $I4_1/a$) (Kruger & Reynhardt, 1978). It does not undergo any phase transition between helium temperature and about 400 K, but its thermal-expansion behavior is remarkable (Brown, Smeltzer & Heyding, 1976; Segel, Karlsson, Gustavson & Edstrom, 1985). The unit cell expands along the *c* axis, but contracts along the *a* axis, so that the unit-cell volume hardly changes even though the axial expansion coefficients are much larger than in the isostructural potassium perrhenate. There have been several structural studies, by single-crystal X-ray diffraction (Kruger & Reynhardt, 1978) and powder neutron diffraction (Brown, Segel & Dolling, 1980), but a more systematic study is needed because of the large temperature-dependent changes in the